Investigations into the cure of model anaerobic adhesives using dielectric spectroscopy

Brendan P. McGettrick and Jagdish K. Vij*
Department of Microelectronics and Electrical Engineering, University of Dublin, Trinity College, Dublin 2, Ireland

and Ciaran B. McArdle
Loctite (Ireland) Ltd, Research and Development Laboratories, Chemical and Materials Science Department, Whitestown Industrial Estate, Tallaght, Dublin 24, Ireland
(Received 1 March 1993; revised 28 July 1993)

The results of investigations into the cure of model anaerobic adhesives by measurements of the real and imaginary parts of the complex permittivity as a function of the cure time are reported. These adhesives are designed to exhibit heterogeneous cure which is initiated by the surfaces of two substrates on either side of a bondline. This situation is referred to as low cure through volume (CTV) or heterogeneous cure. Three stages in the cure process are identified and discussed. A physical model based on the Maxwell–Wagner interfacial polarization effect is given which satisfactorily explains the changes in the complex permittivity which occur due to the surface initiated redox cure of an anaerobic adhesive. The physical model is modified to explain the cure of another model anaerobic adhesive which is deliberately tailored to exhibit a much more homogeneous cure or high CTV. The model is found to fit the experimental data on the complex permittivity for frequencies up to 10 kHz.

(Keywords: complex permittivity; dielectric spectroscopy; anaerobic adhesive)

INTRODUCTION

Dielectric spectroscopy has been used to study chemical reactions for some 60 years. Kienle and Race[1] reported a study of polyesterification reactions using dielectric measurements in 1934. The effects of ionic conductivity on the dielectric properties of the reactants were also discussed. A correlation was found between the viscosity and the conductivity at the initial stages in cure. At the gel stage however, an abrupt change in the viscosity was not followed by a similar change in the conductivity which indicated that the mobility of ions continued to change gradually through the gelation stage. The possibility of electrode polarization occurring at low frequencies was also considered. These phenomena are to be seen in much of the subsequent literature on thermosetting systems.

Between the period of 1934 and 1958 the literature is concerned mainly with the conductivity studies. Work by Fineman and Puddington[2,3] showed correlations between the conductivity and the reaction rate in different resin systems. Since 1958, the increasing practical importance of thermosetting resins has provided an impetus for extensive research into the cure of many materials. Reported work has primarily been concentrated on the study of epoxies and, to a lesser degree, polyesters, polymides and other resins. It is apparent from the literature that many difficulties arise in the application of dielectric measurements to the study of cure. No comprehensive model of dielectric phenomena during cure, that includes the proper chemical kinetics and the correct relations between the state of cure, the temperature and the various dielectric parameters, has been developed. Work along these lines is still ongoing[4–31]. This work has been greatly facilitated with the availability of computer controlled instrumentation such as the Hewlett Packard HP4192A low frequency impedance analyzer, the Schlumberger SI 1255 frequency response analyzer and the Genrad 1689 Digibridge[4].

The object of this study is to characterize the cure behaviour of surface initiated anaerobic adhesives which are formulated to exhibit different levels of cure through volume (CTV) or cure heterogeneity. It is shown that dielectric spectroscopy is one of the most informative methods for this study.

EXPERIMENTAL

The two anaerobic adhesives used were model formulations designed by the Research and Development Laboratories of Loctite (Ireland) Ltd to exhibit different levels of CTV performance. *Table 1* illustrates the ingredients used in these formulations. The low CTV formulation, referred to as CTV1 and the high CTV formulation, CTV2, contained different levels of the same ingredients. The names CTV1 and CTV2 are code names and do not imply any specific characteristics. The accelerating additive was different for each system. CTV1

* To whom correspondence should be addressed

0032-3861/94/05/0939–10

Table 1 Ingredients for a typical anaerobic adhesive formulation

Ingredient	Parts per 100 (by weight)
Hydroxy propyl methacrylate	10.0
Acrylic acid	10.0
Stabilizers	1.4
Saccharin	0.6
Accelerating additive	1.0
Resin base	75.0
Cumene hydroperoxide	2.0

employed acetyl phenyl hydrazine (APH) while the additive used in CTV2 is of a proprietary nature but is referred to by the code name BPH. The nature of the accelerating additive in CTV2 necessitated the use of a primer to activate the substrate in order to achieve cure. The primer was a commercially available copper salt based activator, known as Primer N (Loctite, Welwyn Garden City, UK). The role of the copper primer and its effect on the dielectric properties of the CTV2 samples is discussed in the Results and Discussion section. It is important to note that these curing systems were selected because they simply exhibit different levels of CTV. They are thus suitable for investigation in the development of analytical methods for the study of the CTV phenomenon in anaerobic adhesives.

Dielectric measurements were made using a Hewlett Packard HP4192A impedance analyzer interfaced with a Hewlett Packard Vectra QS/165 PC. Adhesive samples were placed between flat hard tempered iron electrodes of 0.5 mm thickness (Goodfellow Metals, Cambridge, UK; FE000405/11). The base electrode was 30 mm in diameter and the upper electrode was 15 mm in diameter. The effective working electrode area was 177 mm^2. The spacing between electrodes was set using uniform cross-linked polystyrene microbeads with well-characterized diameters (Bangs Laboratories Inc., Carmel, USA). This disposable arrangement was placed in a three terminal dielectric cell similar to that designed by Kremer *et al.*[32]. The temperature of the cell was maintained at 25 ± 0.5°C using a home-made gas temperature control system.

Measurements of the real part of the complex permittivity, ε' and of the imaginary part, ε'', in the frequency range 100 Hz–10 MHz were made as a function of cure time up to 100 h on the formulations CTV1 and CTV2. Two thicknesses of 250 and 650 μm were examined for each formulation. For the high CTV formulation, CTV2, the iron electrodes were primed using Primer N. Due to an inverse proportionality between the capacitance and the thickness it was necessary to increase the working electrode area for the case of 650 μm thick systems. The empty cell capacitance, C_0, of a 650 μm thick, 177 mm^2 working area sample was found to be outside the working range of the HP4192A analyzer ($C_0 = 2.4$ pF). The working area was increased to 707 mm^2 using a 30 mm diameter top electrode.

Plots of the real and imaginary parts of the complex permittivity, ε' and ε'', at frequencies of 100 Hz, 1 kHz, 10 kHz, 100 kHz, 1 MHz and 10 MHz as a function of cure time were constructed for each formulation and thickness. The data were analysed in terms of a Maxwell–Wagner interfacial polarization model and a satisfactory fit of the theoretical model predictions to the data was obtained.

RESULTS AND DISCUSSION

Plots of ε' and ε'' at frequencies of 100 Hz, 1 kHz, 10 kHz, 100 kHz, 1 MHz and 10 MHz as a function of cure time for CTV1 are illustrated in *Figures 1* and *2*. Three stages in the cure process are evident and are discussed under the following headings: the induction stage; the activation

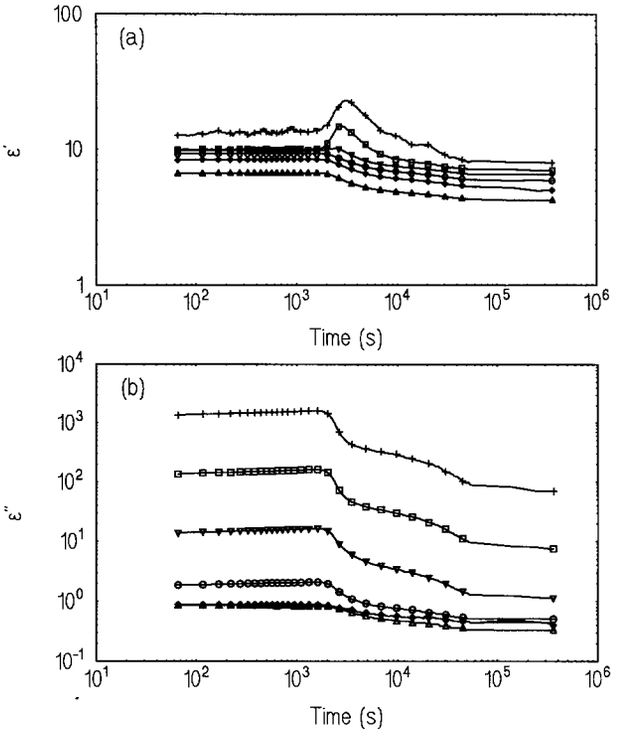

Figure 1 Dielectric data on the 250 μm thick CTV1 sample. Plots of (a) the relative permittivity, ε' and (b) dielectric loss, ε'' *versus* the cure time at frequency of 100 Hz (+), 1 kHz (□), 10 kHz (▽), 100 kHz (○), 1 MHz (◇) and 10 MHz (△)

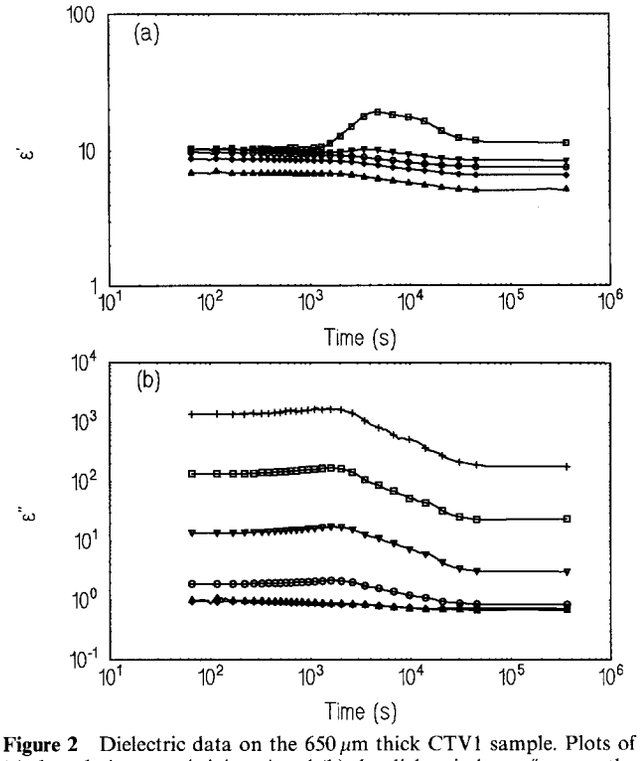

Figure 2 Dielectric data on the 650 μm thick CTV1 sample. Plots of (a) the relative permittivity, ε' and (b) the dielectric loss, ε'' *versus* the cure time at frequencies of 100 Hz (no data), 1 kHz (□), 10 kHz (▽), 100 kHz (○), 1 MHz (◇) and 10 MHz (△)

stage; and the end reaction stage. The anaerobic adhesive cure mechanism is also discussed. Later, a physical model is presented which has been developed to describe and indeed predict to a certain extent the changes in the complex permittivity which occur during the cure of a surface initiated anaerobic adhesive. The physical model is also applied to the high CTV formulation, CTV2. Unsatisfactory correlation at low frequencies between the experimental and the predicted data requires that the model be modified to obtain a good fit. Details of this modification and illustrated comparisons between the experimental and the theoretical data from the model are presented.

The anaerobic adhesive cure mechanism

Anaerobic adhesives are single component acrylic adhesives which cure by a free radical mechanism in the absence of air. They are employed in mechanical engineering applications such as threadlocking, sealing and impregnation. The oxygen inhibition of polymerization means that the formulations must be stored in an aerobic environment such as oxygen-permeable polyethylene containers.

Anaerobic adhesives were developed by Krieble[33] in 1959. At that time their main components were methacrylate monomers, amines and hydroperoxides. Here, the amine and hydroperoxide work together to provide a free radical flux on demand. The decomposition of hydroperoxide in the presence of amine is well known to be catalysed by transition metals, in particular copper[34]. Although many developments have been made, the majority of anaerobic adhesives used nowadays still use cure packages based on tertiary amines, benzoic sulfimide (saccharin) and/or hydroperoxides. A comprehensive overview of anaerobic compositions has recently been published by Boeder[35].

The cure process is thought to proceed by surface initiated free radical polymerization[36,37]. Okamoto[37] has recently published studies of anaerobic cure using two different cure packages. The first study concerns a system comprising of methyl methacrylate (MMA) monomer and a cure package consisting of *N,N*-dimethyl-*p*-toluidine (DMPT), benzoic sulfimide (BS) and cumene hydroperoxide (CHP). The polymerization is shown to proceed at a faster rate at higher temperatures. The calculated activation energy of the polymerization system is found to be 43.5 kJ mol^{-1} which is roughly half the typical value of a thermally initiated free radical polymerization (90 kJ mol^{-1}). It is thus postulated that the polymerization proceeds by redox radical polymerization. It is this low activation energy which enables an anaerobic adhesive to cure at or below room temperature. The reducing agent of this redox initiating system is speculated to be a charge-transfer complex of DMPT and BS. Surprisingly, the role of the oxidizing agent is not assigned to CHP even though the presence of a small amount of CHP has an accelerating effect on the polymerization.

The second study discusses the acetyl phenyl hydrazine (APH)-BS-CHP curing system. This system is similar to that used in the low CTV formulation, CTV1. It is found that the APH-BS-CHP system is much slower than DMPT-BS-CHP and has a long induction time. A copper catalyst is thus used to speed up the reactions. This copper diffuses into the bulk adhesive where it participates in a redox reaction. The activation energy of polymerization is reduced and the polymerization is accelerated. *Scheme 1* typifies a redox initiated free radical polymerization of conventional (alkyl) acrylates. Stages a and b illustrate the redox catalytic cycle. Here Cu^{2+} is reduced to Cu^{+} (stage a) and the latter species decomposes the CHP to generate an initiating radical flux and is thus oxidized to Cu^{2+} (stage b) which is subsequently recycled. The conventional radical initiation of (alkyl) acrylates is illustrated in stage c. Here R represents a proton or a lower alkyl group and R′ is typically a lower alkyl.

Thus, APH and CHP behave as a reducing and oxidizing agent, respectively (i.e. a redox system) and copper acts as a catalyst. The accelerating effect of copper has recently been shown by two of the authors[31]. This redox reaction generates the cumyloxy radical necessary to initiate the MMA addition polymerization. BS is found to behave as a catalyst to shorten the induction time. The long induction time is attributed to the APH reaction products which may behave as free radical inhibitors.

Since the cure initiation is surface catalysed and thin bondlines reduce the diffusion rate of reaction inhibiting oxygen, cure homogeneity is favoured by a small gap between the substrates (of the order of 10 μm)[30,31]. In situations of thick bondlines, the bulk adhesive in the centre of the bondline will not reach full cure. This may arise due to the physical barrier to metal ion diffusion into the bulk from the substrate caused by a cured adhesive layer adjacent to the substrate. Heterogeneous cure or poor CTV results and bonds with poor or low CTV performance exhibit poor mechanical properties. To probe this CTV–bondline thickness relationship, two thicknesses of 250 and 650 μm are investigated in this work.

The cure systems under investigation, CTV1 and CTV2 with copper primer were designed to exhibit different degrees of cure heterogeneity of CTV performance so that the influence of the bondline thickness and the formulation variables may be assessed. Thus, CTV1

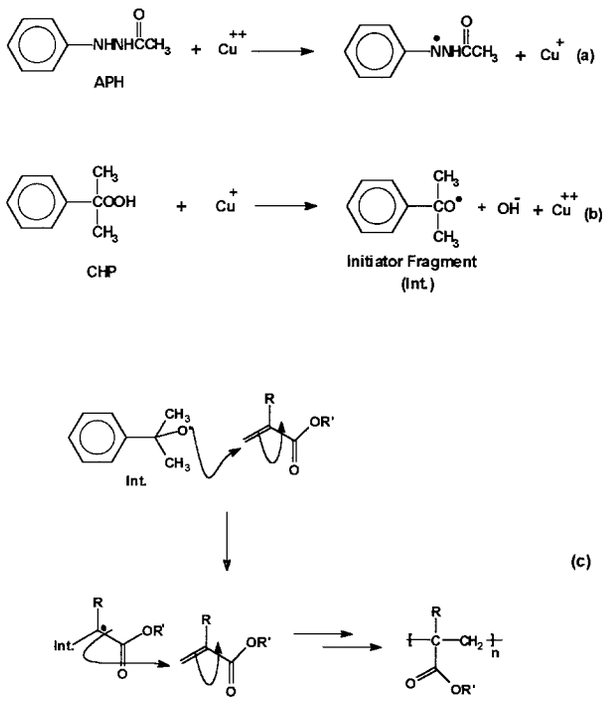

Scheme 1

exhibits a high level of cure heterogeneity or low CTV performance and CTV2 with copper primer exhibits a low level of cure heterogeneity or high CTV performance. *Figures 1* and *2* illustrate the measured changes in dielectric properties with cure time of the low CTV formulation, CTV1. This formulation employs an APH-BS-CHP cure engine as described by Okamoto[37] above. These plots allow analysis of the cure in real time. The three stages in the cure process are discussed below.

The induction stage is the initial period of time during which there is negligible change in ε' and a small rise in ε''. Thus, no significant change in the physical properties of the material is discernible and the crosslinking has not commenced. This induction stage may be due to the time dependent depletion of the reaction inhibiting oxygen from the sample. Alternatively, it may be linked to the finite time which is necessary for the formation of the critical free radical concentration required to initiate cure. The small rise in ε'' is attributed to an increase in the d.c. conductivity of the sample as cure progresses through the induction stage. This rise in d.c. conductivity could arise from the formation of charge carriers. One source for these charge carriers may arise due to the catalytic activity of BS as discussed by Okamoto[37]. Okamoto proposes the reaction shown in *Scheme 2*. Here, the proton H^+ from BS may attack the oxygen of CHP to form the intermediate, compound **1**. The intermediate, **1**, may form a cumyl cation and hydrogen peroxide. This reaction is an equilibrium reaction and the equilibrium can often be forced towards the formation of the cation and the peroxide under mildly acidic conditions.

Okamoto also proposes an explanation for the induction stage in APH-BS-CHP systems by considering the partial conversion of APH to compound **2** which has a hydroxyamine structure (*Scheme 3*). Such a species may behave as a good radical inhibitor and thus moderate the concentration of initiating species[37].

Analysis of *Figures 1* and *2* shows that the induction times are similar for the two thicknesses, 250 and 650 μm. This would indicate that the induction stage is independent of the sample geometry. We thus attribute the induction stage to some type of chemical activity which occurs at the substrate adhesive interface and is independent of specimen geometry. Further evidence of this may be found in a previous publication by two of the authors which illustrates the accelerating effect of copper[31]. Here, the substrates are primed with a copper primer. These primed samples show no induction stage indicating it is less than the time required to assemble the test cell and commence measurements. This demonstrates both the accelerating effect of copper and the effect of altering the substrate adhesive interface on the induction time.

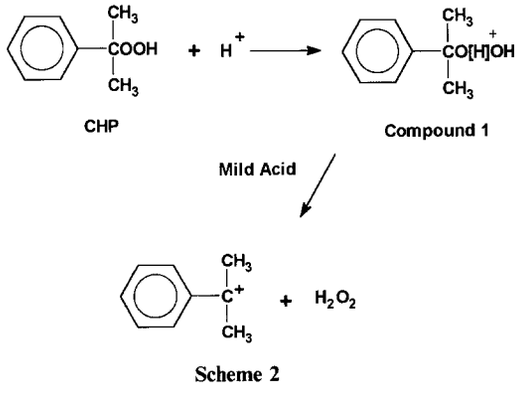

Scheme 2

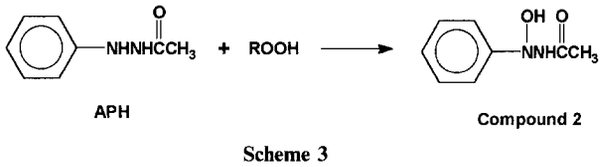

Scheme 3

The activation stage is defined as the period during which ε' and ε'' change significantly with time. Typical results from the literature show a decrease in ε' and ε'' during this stage. We report a significant rise in ε' which results in a peak followed by a decrease and a large drop in ε''. This peak in ε' is greater at lower frequencies and is especially predominant for thicker layers. A similar phenomenon was reported recently in cure studies of rubber filled epoxy resins[23–26]. These rubber filled epoxy resins are known to undergo phase separation during cure[38–43]. The observed dielectric effect was thus attributed to interfacial polarization occurring between the two different phases of differing conductivity. This can give rise to a so-called Maxwell–Wagner absorption[43–45]. In theory, a concurrent increase in both ε' and ε'' to a peak followed by a decrease may be observable as described by Mangion and Johari[22]. The peak in ε' can be masked in some cases by electrode polarization effects leading to a large double layer capacitance contribution to the measured ε'. The peak in ε'' can also be masked in some cases by the relatively large contribution from the d.c. conductivity of the curing resin to the measured ε''. The latter may account for the absence of the ε'' peak associated with the Maxwell–Wagner interfacial polarization absorption in some of the literature[24–26]. The change in the dielectric properties which take place during the cure of the surface initiated anaerobic adhesive can be explained quantitatively in terms of the Maxwell–Wagner interfacial polarization model[43–45]. This physical model is discussed later.

Comparison between the conductivity and the viscosity measurements has revealed that at low frequencies the conductivity, σ, tracks reciprocally the build-up in viscosity as the reaction advances[8,9,46]. The fall in conductivity due to increasing viscosity may be explained as follows: ε'' is a function of the ionic conductivity, the dipole polarization and the electrode polarization. If the ionic conductivity term, σ, dominates then ε'' is dependent on ω^{-1}. At low frequencies, ε'' is dominated by σ as follows:

$$\varepsilon'' = \frac{\sigma}{\omega \varepsilon_0} \tag{1}$$

where ω is the angular frequency ($\omega = 2\pi f$) and ε_0 is the permittivity of free space ($\varepsilon_0 = 8.854\ \mathrm{pF\ m^{-1}}$). In terms of the number of ions per unit volume N with a charge q and a mobility μ, σ can be expressed by:

$$\sigma = Nq\mu \tag{2}$$

μ is related to the dynamic viscosity of the medium, η by the following equation which may be derived from Stokes law:

$$\mu = \frac{q}{6\pi\eta R} \tag{3}$$

where R is the radius of the ion. The ionic mobility in a resin depends primarily on the mobilities of the polymer segments. During cure, the polymer segment mobility is impeded due to the formation of a three-dimensional macroscopic molecular network. The ionic mobility is thus impeded and the ionic conductivity drops. Thus, a measure of the conductivity in a cured polymeric sample gives a good indication of the degree of cure in the sample. Since the specific conductivity, σ, is a bulk property which is independent of the specimen geometry, the initial low frequency values of ε'' are therefore independent of the sample thicknesses.

During the activation stage, ε'' is observed to drop by several orders of magnitude. Gotro and Yandrasits[8] have interpreted this rapid change in ε'' as a qualitative indicator of the onset and the speed of cure. At the early stages of the cure when the conductivity is high the following relationship holds:

$$\frac{d(\log \varepsilon'')}{dt} \propto \frac{d(\log \sigma)}{dt} \quad (4)$$

During the activation stage the plots illustrate a greater slope or rate of change of ε'' for the thinner layers. This indicates that the cure rate is dependent on the adhesive layer thickness. The plots show that the cure proceeds at a faster rate in the thinner layers compared to the thicker layers.

The end reaction stage involves a slow decrease in ε' and ε'' with time. ε' and ε'' eventually reach stable values and will not change under the isothermal conditions. Now, it is assumed that the material will not cure any further unless cure conditions are altered, e.g. heat applied to the system. We note the absence of a peak in ε'' during this 'flattening off' stage as observed by others in studies of epoxy/amine curing systems[4,6,10,14–26]. This peak is associated with a dipolar reorientation process which arises due to the rotational motion of the pendant hydroxyl (OH) group which is generated as a consequence of the epoxy/amine curing reaction[23]. In the case of the anaerobic acrylic adhesives under investigation here, we postulate that any manifestation of a dipolar reorientation process, such as a peak in ε'', would be masked by the large contribution of the d.c. conductivity of the curing resin to the measured ε''. Indeed, Mangion and Johari[22] have shown that increasing the d.c. conductivity by raising the cure temperature renders the peak in ε'' associated with the dipole reorientation process unobservable.

The physical model

The model is based on the Maxwell–Wagner effect. This effect may arise when a dielectric material of low conductivity contains a dispersed phase of differing (conventionally higher) conductivity. Electric charge can migrate through the conducting phase to the interface between it and the low conductivity phase. This interfacial polarization causes a dielectric phenomenon which is manifested as an increase in the dielectric permittivity, ε' and the dielectric loss, ε''[23].

We model the anaerobic adhesive cure system by considering three stages during the crosslinking process. *Figure 3* illustrates these three stages. At stage 1, no cure has taken place in the adhesive of thickness, d. At stage 2, the cure has progressed from the substrate inwards by a distance $(d-\delta)/2$ from each side. At stage 3, the sample

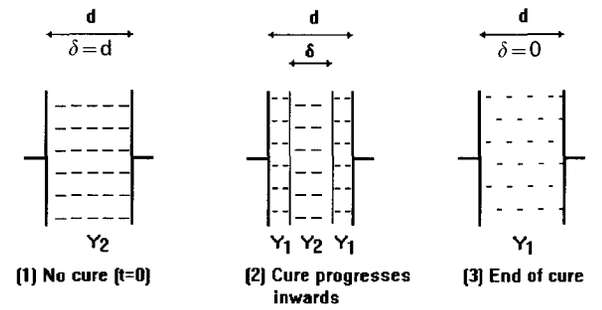

Figure 3 Schematic representation of the three stages in the cure process of the low CTV performance surface initiated anaerobic adhesive formulation, CTV1. Thickness of the uncured layer, δ, goes down from d (completely uncured sample) to zero (fully cured sample) as cure progresses

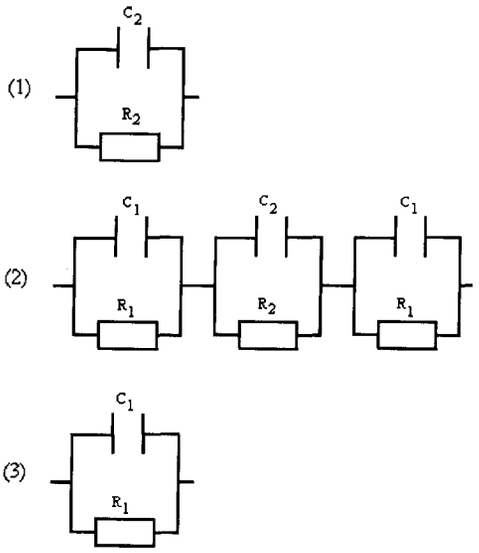

Figure 4 Electrical circuit representation of the three stages in the cure process of the low CTV performance surface initiated anaerobic adhesive formulation, CTV1. C_1 and C_2 are variable capacitances defined by: $C_1=\varepsilon_0\varepsilon_1 A/(d-\delta)/2$; $C_2=\varepsilon_0\varepsilon_2 A/\delta$

is fully cured and $\delta=0$. This model excludes the possibility of the creation of additional electric charge from the chemical reaction or during the polarization of the system. The system in *Figure 3* may be electrically represented by three electrical circuits as illustrated in *Figure 4*. C_2 and R_2 are the capacitance and resistance, respectively, of the uncured adhesive. C_1 and R_1 are the capacitance and resistance, respectively, of the cured resin. These equivalent circuits do not account for the fact that ε' increases with decrease in the measurement frequency, ω. This behaviour is accounted for by inputting the initial (cure time = 0) and the final ($t=t_{cured}$) values of the permittivity, ε', at each measurement frequency into the mathematical equation for the physical model which is developed below in equations (5) to (13). It is also important to note that in the case of copper primed substrates (for CTV2), the copper ions diffuse into the bulk adhesive where they participate in a redox reaction. It was thus assumed that the copper ions do not form a blocking layer or a double layer of charged ions at the electrodes. This assumption was verified by analysing the dielectric properties of CTV2 without the copper primer. Here the initial values of ε' and ε'' for CTV2 without the primer were similar to those for CTV2 with the primer. CTV2 without the copper primer did not cure however.

The total admittance, Y_T, of the curing system in stage

2 may be written using Ohm's law:

$$\frac{1}{Y_T} = \frac{2}{Y_1} + \frac{1}{Y_2} \tag{5}$$

where Y_1 is the admittance of the cured layer and Y_2 is the admittance of the uncured layer. Y may be expressed in general terms as follows:

$$Y = i\omega C^* = G + i\omega C \tag{6}$$

where C^* is the complex capacitance of the sample, G is the conductance ($G = R^{-1}$) and C is the capacitance of the entire system. Thus:

$$Y_1 = \frac{A\sigma_1}{\frac{d-\delta}{2}} + \frac{i\omega\varepsilon_0\varepsilon_1 A}{\frac{d-\delta}{2}} \tag{7}$$

where A is the electrode area, σ_1 is the specific conductivity of the cured layer, d is the separation between the electrodes, δ is the thickness of the uncured layer and ε_1 is the permittivity of the cured sample. Also:

$$Y_2 = \frac{A\sigma_2}{\delta} + \frac{i\omega\varepsilon_0\varepsilon_2 A}{\delta} \tag{8}$$

where σ_2 is the specific conductivity of the uncured layer and ε_2 is the permittivity of the uncured specimen. Substitution of equations (6), (7) and (8) into equation (5) yields:

$$\frac{1}{i\omega C^*} = \frac{2}{\frac{a\sigma_1 + i\omega\varepsilon_0\varepsilon_1 A}{\frac{d-\delta}{2}}} + \frac{1}{\frac{A\sigma_2 + i\omega\varepsilon_0\varepsilon_2 A}{\delta}} \tag{9}$$

and

$$\frac{1}{i\omega C^*} = \frac{2}{\left(\frac{i\omega\varepsilon_0 A}{\frac{d-\delta}{2}}\right)\left(\varepsilon_1 - \frac{i\sigma_1}{\varepsilon_0\omega}\right)} + \frac{1}{\left(\frac{i\omega\varepsilon_0 A}{\delta}\right)\left(\varepsilon_2 - \frac{i\sigma_2}{\varepsilon_0\omega}\right)} \tag{10}$$

On rearranging equation (10) we obtain:

$$\frac{1}{C^*} = \frac{1}{\left(\frac{\varepsilon_0 A}{d-\delta}\right)\left(\varepsilon_1 - \frac{i\sigma_1}{\varepsilon_0\omega}\right)} + \frac{1}{\left(\frac{\varepsilon_0 A}{\delta}\right)\left(\varepsilon_2 - \frac{i\sigma_2}{\varepsilon_0\omega}\right)} \tag{11}$$

C^* can be expressed in terms of the real and imaginary parts of the complex permittivity using the equation:

$$C^* = \frac{\varepsilon_0(\varepsilon' - i\varepsilon'')A}{d} \tag{11a}$$

where ε' and ε'' are the observed values of the real and imaginary parts of the complex permittivity of the system. For frequencies approximately below 10 kHz, the d.c. conductivity is the dominant contributor to the dielectric loss, ε''. Thus, the model is fitted to the data in the frequency range, 100 Hz–10 kHz.

One of the main difficulties of comparing the results from equation (11) with those obtained experimentally is that the dependence of $(d-\delta)$ on time is unknown. From a practical point of view it is important to determine the dependence of $(d-\delta)$ on time. In order to determine this dependence the following analysis is proposed. In equation (11), σ_1 and σ_2 represent the specific conductivities of the cured and uncured layers of the adhesive, respectively. Since σ_1 is unlikely to reach a constant value immediately it is assumed that it decreases with increase in $(d-\delta)$ as:

$$\sigma_1 = \sigma_2 \exp\left[\frac{-(d-\delta)}{\tau}\right] \tag{12}$$

i.e. σ_1 is assumed to decay exponentially with an increase in $(d-\delta)$ and τ is the value of $(d-\delta)$ at which σ_1 has dropped to $\exp^{-1}$ or to 37% of its initial value. When $(d-\delta) = 2.2\tau$, σ_1 has decayed from 90 to 10% of its original value. Equation (12) satisfies the initial condition, for $t = 0$; $(d-\delta) = 0$. σ_1 is now defined as the specific conductivity of the curing resin layer and not of the fully cured resin layer as defined previously. Equation (11) thus becomes:

$$\frac{1}{C^*} = \frac{1}{\left(\frac{\varepsilon_0 A}{d-\delta}\right)\left\{\varepsilon_1 - \frac{i\sigma_2 \exp\left[\frac{-(d-\delta)}{\tau}\right]}{\varepsilon_0\omega}\right\}} + \frac{1}{\left(\frac{\varepsilon_0 A}{\delta}\right)\left(\varepsilon_2 - \frac{i\sigma_2}{\varepsilon_0\omega}\right)} \tag{13}$$

Using equation (11a), we can determine ε' and ε'' of the entire system using a computer program. We input the measured values of ε_1 and ε_2 at each frequency, σ_2, A, d and ω and vary τ to get the best fit to the experimental data.

Comparison of the model to the experimental results

Figure 5 illustrates the fit of this physical model to the data for the 250 μm thick CTV1 sample. We obtain a similar fit for the 650 μm CTV1 sample. The values of τ used are presented in *Table 2*. Comparison between the

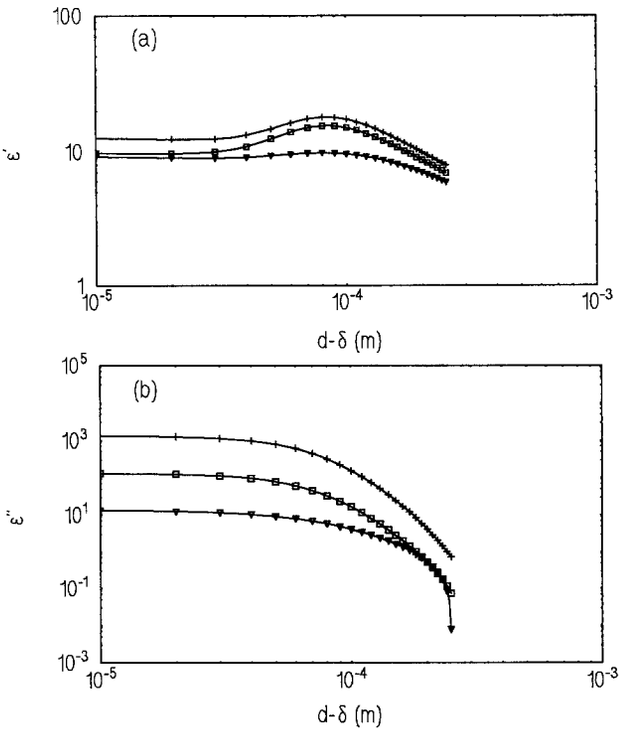

Figure 5 Predicted dielectric data from the physical model for the 250 μm thick CTV1 sample. Plots of (a) the relative permittivity, ε' and (b) the dielectric loss, ε'' *versus* $(d-\delta)$ at frequencies of 100 Hz (+), 1 kHz (□) and 10 kHz (▽)

experimental data of *Figures 1a* and *2b* and that predicted by the model illustrated in *Figures 5a* and *b* show that the model along with the suggested conductivity decay procedure fits the measured values of ε' and ε'' reasonably well. We discuss this in terms of the three stages discussed earlier; the induction stage, the activation stage and the end reaction stage.

Figures 5a and *b* illustrate the predicted changes in the dielectric properties of the sample as the cure emanates inwards from the substrate surface, i.e. as $(d-\delta)$ increases from 0 to d. Previously, the various stages in the cure were discussed as a function of the cure time. We now discuss these stages in terms of the two curing layers which move inwards from the substrate surfaces and the uncured layer. The plots illustrate two stages, the induction and the activation stages.

The fact that an induction stage is present in the data from the physical model indicates that this stage may not be purely time dependent as discussed earlier. It appears that for each CTV1 sample there is a critical value of $(d-\delta)$ above which the dielectric permittivity, ε', starts to rise due to an interfacial polarization effect between an uncured layer of high conductivity, σ_2 and two curing layers of lower conductivity, σ_1. The model predicts a higher critical value of $(d-\delta)$ for greater sample thicknesses. *Figures 1* and *2* show the induction stage is independent of the sample thickness. This is in contrast to our calculations using the model. We conclude therefore, that while the induction stage appears to be thickness independent and substrate–adhesive interface dependent it also involves some critical value of the depth of cure, $(d-\delta)$.

The activation stage is seen after the induction stage. As observed in *Figures 1* and *2* ε' rises to a maximum and then falls to a lower value than before. The height and width of this peak is dependent on the initial conductivity of the uncured system σ_2, the sample thickness, d and the exponential decay constant, τ. It was observed that by inserting various values of σ_2 into the model the peak height increased with increase in σ_2 and the peak height and width increased with increase in d. However, since σ_2 and d are experimentally obtained values we vary only τ to get the best fit. This peak in ε' is accompanied by a rapid drop in ε'' as observed experimentally. It is concluded that this behaviour is mainly due to the Maxwell–Wagner interfacial polarization between the uncured layer of high conductivity, σ_2 and the two curing layers of lower conductivity, σ_1.

No end reaction stage is visible in the data predicted by the model. This is because experimentally, the end reaction stage involves the time during which the conductivity of the sample has decreased to a very small value. The contributions to the complex permittivity will now arise from the dipoles of the system. The gradual fall in ε' and ε'' during this stage is thus due to the gradual immobilization of polar groups arising from the slow increase in viscosity as the cure comes to an end. This stage cannot be easily accounted for in such a model.

Table 2 Values of τ and C_d for the different thicknesses obtained for the CTV1 and the CTV2 formulations

Formulation	d (μm)	τ (μm)	C_d (μF)
CTV1	250	25	–
CTV1	650	133	–
CTV2	250	24	6
CTV2	650	63	50

The modified physical model

Figures 6 and *7* illustrate the measured change in the complex permittivity of the high CTV formulation, CTV2, as a function of cure time. Comparison of these plots with those for CTV1 in *Figures 1* and *2* shows that CTV2 with copper primer has a much higher initial conductivity than CTV1 (by almost two orders of magnitude). This initial high conductivity is conferred by the presence of the accelerating additive BPH. The influence of the copper primer on the initial dielectric properties was found to be insignificant as described above. Also, at low frequencies CTV2 exhibits a very large dielectric permittivity, $\varepsilon'(>10^3)$, which is not observed for CTV1. This large value of ε' at low frequencies is typical of a double layer effect[4,5,47]. This phenomenon is well known and will only be briefly discussed.

For the low alternating voltages that are normally used for dielectric measurements, the electrode–resin interface acts as an electrochemical barrier to the flow of ions. The application of an electric field can cause the accumulation of the ion layers which can lead to electrode polarization or a 'double layer'. In effect this can be represented as a capacitor in series with the test sample. The layer has a relatively low permittivity but the extreme thinness (of the order of a few ångströms) of the layer leads to a very large capacitance per unit area. The double layer capacitance can be very high and may dominate the overall measured low frequency dielectric permittivity when the conductivity is large ($\varepsilon' > 10^3$), e.g. during the early stages of cure. For longer cure times, the conductivity is diminished and the double layer capacitance will

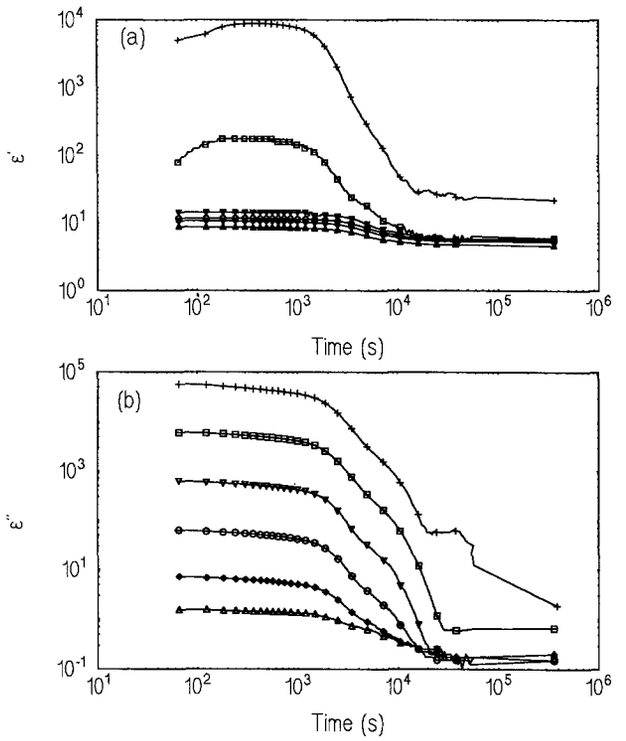

Figure 6 dielectric data on the 250 μm thick, N primed CTV2 sample. Plots of (a) the relative permittivity, ε' and (b) the dielectric loss, ε'' *versus* the cure time at frequencies of 100 Hz (+), 1 kHz (□), 10 kHz (▽), 100 kHz (○), 1 MHz (◇) and 10 MHz (△)

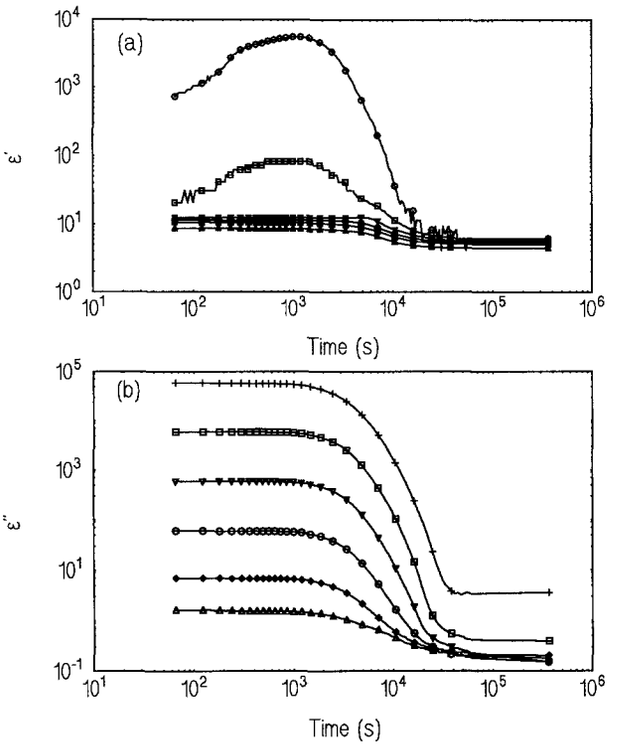

Figure 7 Dielectric data on the 650 μm thick, N primed CTV2 sample. Plots of (a) the relative permittivity, ε' and (b) the dielectric loss, ε'' *versus* the cure time at frequencies of 100 Hz (+), 1 kHz (□), 10 kHz (▽), 100 kHz (○), 1 MHz (◇) and 10 MHz (△)

have little effect on the overall measured capacitance or on the dielectric permittivity of the sample. To test this double layer hypothesis we modify the physical model. The modification simply involves adding in a double layer capacitance, C_d in series with the circuits shown in *Figure 4*. We define C_d as the double layer capacitance which is formed due to the time dependent build up of charged species at the electrodes. C_d is calculated at zero cure time. A more refined physical model would account for this time dependent build up of charge by expressing C_d as a function of time. Indeed, the experimental results in *Figures 6a* and *7b* indicate that the apparent double layer capacitance observed at the lower frequencies increases with cure time during the induction stage. The modified circuits are thus similar to those in *Figure 4* except for an additional empirical double layer capacitance C_d in series with each circuit. The inverse complex capacitance of the modified model can be written as equation (13) with the additional term $(1/C_d)$ added to the right-hand side.

We now have two adjustable parameters, τ and C_d for the model. It is important to note that the low frequency values of ε_2 (0.1 and 1 kHz) were not taken directly from the measured data because these appeared to be influenced by double layer effects. Instead, values close to those obtained at 10 kHz were used because at higher frequencies the capacitive reactance offered by the relatively large double layer capacitance is negligible. The double layer effect is thus unobservable at these higher frequencies. τ and C_d were varied until the closest fit to the results was obtained. The results of this fitting for the 250 μm thick copper primed CTV2 sample are illustrated in *Figure 8*. We obtain a similar fit for the 650 μm sample. The values of τ and C_d used are presented in *Table 2*. From C_d, we can determine the thickness of the double layer provided an assumption about the value of its dielectric permittivity can be made[5,47].

The fit of the modified physical model to the experimental data of *Figures 6a* and *b* (CTV2 with copper primer, 250 μm thick) is presented in *Figures 8a* and *b*. The double layer effect is seen at 0.1 and 1 kHz, i.e. ε' is extremely high. The double layer capacitance is greater for the thicker samples than for the thinner samples (6 μF for 250 μm and 50 μF for 650 μm). This is because there is a greater number of ions in thicker layers and thus more effective double layers may be formed in the thicker samples. However, in the experimental data, ε' is seen to rise during the induction stage. This is not seen in the predicted data. We attribute this phenomenon to the gradual formation of a double layer due to the build up of charged species as a function of time at the electrodes. This time dependent charge build up phenomenon is not accounted for in the model. It is important to note that this effect is predominant due to the extremely high conductivity of the CTV2 formulation. It is likely that the CTV1 formulation also has double layers but its relatively low conductivity and hence the lower number density of ions precludes observation of this effect. We observe a peak in ε' at 10 kHz during the activation stage for CTV2 in the predicted data of *Figure 8a* as was observed in CTV1. This peak is not observable at the lower frequencies of 100 Hz and 1 kHz due to the extremely large double layer capacitance the effect of which dominates the measured impedance, especially at low frequencies. This peak is unobservable in the experimental data for the 250 μm CTV2 sample in *Figure 6a* but close scrutiny of the measured data for the 650 μm sample reveals the presence of a peak. We conclude that CTV2 with copper primer does actually undergo the Maxwell–Wagner interfacial polarization effect during

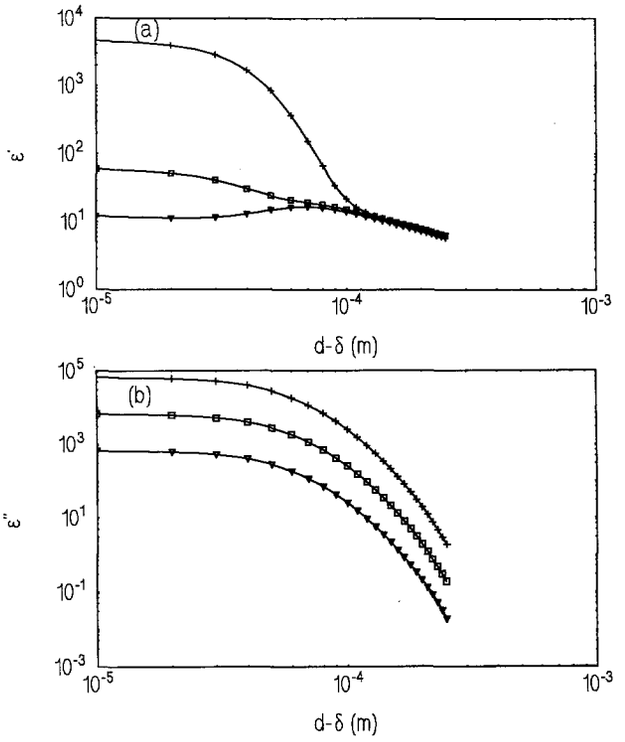

Figure 8 Predicted dielectric data from the modified physical model for the 250 μm thick, N primed CTV2 sample. Plots of (a) the relative permittivity, ε' and (b) the dielectric loss, ε'' *versus* $(d-\delta)$ at frequencies of 100 Hz (+), 1 kHz (□) and 10 kHz (▽)

cure but the dielectric manifestations of this effect are obscured by the electrode polarization effects.

Findings of the analysis with regard to CTV

The main limitation of this model is that it considers only the cases of complete homogeneous cure or high CTV. However, the fact that it fits the experimental data quite well is significant as it provides information on some of the basic concepts of the curing process in anaerobic adhesives. First, the uncured adhesive of high conductivity comes into contact with a suitable surface. Cure is initiated from this surface after a finite time. A layer of curing adhesive emanates from each substrate surface inwards. The specific conductivity of this layer is assumed to decrease exponentially as the curing layer thickness or the depth of cure increases. The satisfactory fit of the model to the experimental data offers some proof for the validity of this assumption. An interfacial polarization phenomenon occurs between the uncured resin of high conductivity and the curing resin of lower conductivity for some critical layer thickness of the latter. The two curing layers eventually meet. The model predicts that the layers meet and form a fully cured homogeneous network with very low conductivity. In practice, the end result is likely to be an adhesive bondline with varying degrees of cure. Adjacent to the substrate the degree of cure is likely to be high. Deeper into the bondline the degree of cure will diminish according to some cure gradient. This gradient may be related to the conductivity changes occurring in the sample. The adhesive bond will therefore never reach a stage of complete cure homogeneity as predicted by the model.

Figure 9 illustrates the fit of $(d-\delta)$ from the physical model to the cure time from the experiments for the low and high CTV performance formulations, CTV1 and CTV2, respectively. An estimate may be obtained from these plots for the extent of cure at a given time for the various samples. The cure profile of $(d-\delta)$ *versus* time is quite similar for CTV1 and CTV2. In both cases, the thicker samples take longer times to cure than the thinner samples. *Figure 9* does not yield any information as to why CTV2 exhibits better CTV performance than CTV1. However, analysis of the previous plots of ε' and ε'' *versus* both time and $(d-\delta)$ may provide some explanation as discussed below.

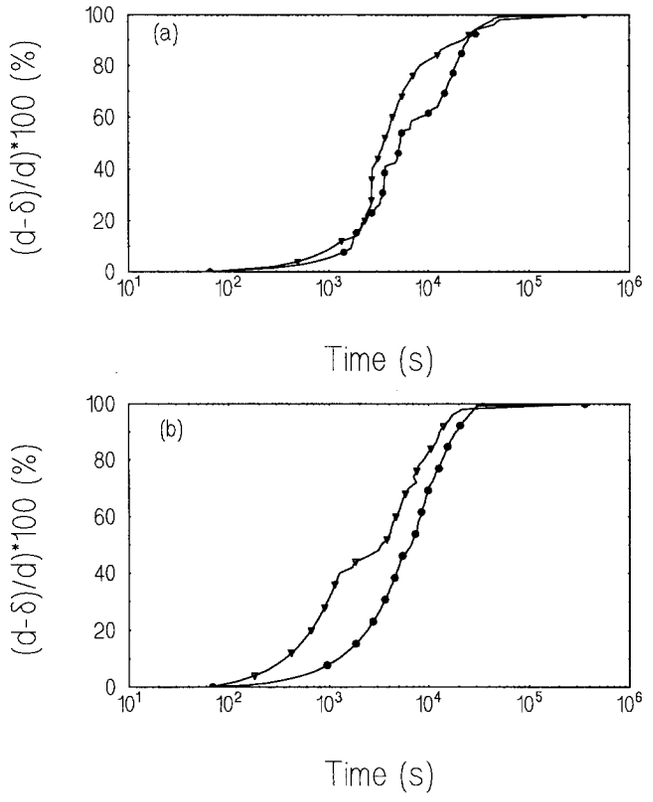

Figure 9 Data from the fitting of $(d-\delta)$ from the physical model to the cure time from the experiments. Plots of $(d-\delta)$ *versus* the cure time for (a) CTV1 and (b) N primed CTV2 for thicknesses of 250 μm (▽) and 650 μm (●)

The judicious choice of the redox active additive BPH confers high conductivity to the CTV2 formulation. This is manifested as an extremely large dielectric loss at low frequencies ($\varepsilon''=74\,000$ at 100 Hz). Also, the calculated values of the conductivity exponential decay constant, τ, are similar for CTV1 and CTV2 for thin samples but for the thick samples the values are much lower for CTV2 ($\tau=63$) than for CTV1 ($\tau=133$). This means that for thicker samples the conductivity decays at a much faster rate during cure in CTV2 than in CTV1. Thus, the high conductivity dominates the complex permittivity during the induction and the activation stages and may play an important role in the creation of a more suitable environment for redox reactions and high CTV performance.

As discussed earlier, a low final conductivity in a cured polymeric sample is indicative of a high degree of cure. It is interesting to note that the final conductivity is one order of magnitude lower for CTV2 than for CTV1. Also, the final conductivities of the thin and thick samples are similar for CTV2 whereas for CTV1 the final conductivity of the thinner sample is almost one order of magnitude lower than for the thicker sample. Thus, it is predicted that the CTV performance would be similar for thin samples of CTV1 and CTV2 whereas for thicker samples, CTV1 would exhibit inferior CTV performance while CTV2 would retain good CTV. *Table 3* illustrates tensile test data for bonded metal lapshear specimens arranged to have bondlines of preset thickness or 'gap'. At zero gap (i.e. an essentially mating substrate situation wherein the adhesive layer thickness is 10 μm or less), CTV1 and CTV2 give comparable performance as might be expected given their comparable polymer forming compositions and the ideal cure conditions (high ratio of surface bound metallic species to adhesive layer volume). At the thick 500 μm gap, the model low CTV formulation, CTV1, exhibits inferior performance to that of model CTV2 which retains high strength as was predicted from the analysis of the conductivity measurements.

The ability to regulate conductivity changes in CTV2 during cure may be linked to its high CTV performance. This is achieved not by merely doping the formulation with a typical conductor, but by choosing appropriate additives that additionally participate in the redox chemistry and operate in synergism with the other

Table 3 Bond strengths and the specific conductivities of the CTV1 and the CTV2 formulations

Formulation	Conductivity (μS m^{-1})	Bond strength (dN cm^{-2})[a]	
		0 mm	0.5 mm
CTV1	7.4	244	31
CTV2	380.0	249	200

[a] Tensile testing according to ASTM D100-64

components of the cure system. In this way, the essential cure components can be used more efficiently with a concomitant improvement in the performance of the model anaerobic adhesive.

Further criteria such as toxicity and compositional stability pertain to additives for formulations which may be further developed but which need not necessarily apply to model anaerobic adhesives. It is gratifying to note that variations of the systems under study show promise in this regard. Concurrent studies using real time Fourier transform infra-red spectroscopy complement the results and the analysis outlined above and these will be reported at a later date.

CONCLUSIONS

Dielectric spectroscopy has been shown to be one of the most useful techniques for examining the process of surface initiated heterogeneous redox polymerization in anaerobic adhesives. Two anaerobic formulations were investigated, one designed to exhibit poor CTV and the other to exhibit high CTV. Three stages in the cure process were identified and discussed: the induction stage; the activation stage; and the end reaction stage.

A physical model has been developed based on the Maxwell–Wagner formalism which describes the anaerobic cure. The predictions of the model are found to be in reasonable agreement with the experimental data for the low CTV formulation, CTV1. For the case of the high CTV formulation, CTV2, the model is modified to include a double layer capacitance, the effect of which arises from the time dependent build of the high number density of charge carriers in the formulation at the electrodes.

Comparison of the data from the physical model and the experimental data provided an understanding of the process of surface initiated anaerobic adhesive cure and its associated dielectric behaviour. The high CTV formulation has been found to have an initial conductivity 50 times higher than the low CTV formulation. Values of the conductivity exponential decay constant, τ, are similar for all thin samples indicating similar CTV performance. For thicker layers however, τ is much lower in the formulation CTV2 than for the formulation CTV1 indicating superior CTV performance in the former. The ability to regulate conductivity changes during the activation stage may be linked to CTV performance. It originates from the judicious choice of a new redox active addivitve, BPH and its interaction with the other components in the cure system.

ACKNOWLEDGEMENTS

The authors thank Professor B. K. P. Scaife and Professor W. G. Scaife both of Trinity College, Dublin, Dr J. Guthrie of Loctite (Ireland) Ltd, Dublin and Dr Y. P. Kalmykov of the Russian Academy of Sciences, Moscow for useful discussions. The authors are also grateful to Loctite Materials Ireland and to EOLAS for funding and for permission to publish this paper.

REFERENCES

1 Kienle, R. H. and Race, H. H. *Trans. Electrochem. Soc.* 1934, **87**, 87
2 Fineman, M. N. and Puddington, I. E. *Ind. Eng. Chem.* 1947, **39**, 1288
3 Fineman, M. N. and Puddington, I. E. *Can. J. Res. B* 1947, **25**, 101; Delmonte, J. *J. Appl. Polym. Sci.* 1959, **2**, 108
4 Senturia, S. D. and Sheppard, N. F. *Adv. Polym. Sci.* 1986, **80**, 3
5 Day, D. R. Lewis, T. J., Lee, H. L. and Senturia, S. D. *J. Adhesion* 1985, **18**, 73
6 Sheppard Jr, N. F. *PhD Thesis* Massachusetts Institute of Technology, 1986
7 Sheppard Jr, N. F. and Senturia, S. D. 'Proc. IEEE Conf. on Electrical Insulation and Dielectric Phenomena', 2–6 November, IEEE, New York, 1986
8 Gotro, J. and Yandrasits, M. *Polym. Eng. Sci.* 1989, **29**, 278
9 Kranbuehl, D., Delos, S., Hoff, M., Haverty, P., Freeman, W., Hoffman, R. and Godfrey, J. *Polym. Eng. Sci.* 1989, **29**, 285
10 Senturia, S. D., Sheppard Jr, N. F., Lee, H. L. and Day, D. R. *J. Adhesion* 1982, **15**, 69
11 Nass, K. A. and Seferis, J. C. *Polym. Eng. Sci.* 1989, **29**, 315
12 Lane, J. W., Seferis, J. C. and Bachmann, M. A. *Polym. Eng. Sci.* 1986, **26**, 346
13 Bidstrup, S. A., Sheppard Jr, N. F. and Senturia, S. D. *Polym. Eng. Sci.* 1989, **29**, 325
14 Mangion, M. B. M. and Johari, G. P. *J. Polym. Sci., Polym. Phys. Edn* 1991, **29**, 1117
15 Mangion, M. B. M. and Johari, G. P. *J. Polym. Sci., Polym. Phys. Edn* 1991, **29**, 1127
16 Mangion, M. B. M. and Johari, G. P. *J. Polym. Sci., Polym. Phys. Edn* 1991, **29**, 437
17 Mangion, M. B. M. and Johari, G. P. *J. Polym. Sci., Polym. Phys. Edn* 1990, **28**, 1621
18 Mangion, M. B. M. and Johari, G. P. *Polymer* 1991, **32**, 2747
19 Mangion, M. B. M., Wang, M. and Johari, G. P. *J. Polym. Sci., Polym. Phys. Edn* 1992, **30**, 433
20 Mangion, M. B. M. and Johari, G. P. *Macromolecules* 1990, **23**, 3687
21 Mangion, M. B. N. and Johari, G. P. *J. Polym. Sci., Polym. Phys. Edn* 1990, **28**, 71
22 Mangion, M. B. M. and Johari, G. P. *J. Polym. Sci., Polym. Phys. Edn* 1992, **30**, 445
23 Wang, M., Johari, G. P. and Szabo, J. P. *Polymer* 1992, **33**, 4747
24 Wang, M., Szabo, J. P. and Johari, G. P. *Polymer* 1992, **33**, 4951
25 Maistros, G. M., Block, H., Bucknall, C. B. and Partridge, I. K. *Polymer* 1992, **33**, 4470
26 Delides, C. G., Haward, D., Pethrick, R. A. and Vatalis, A. S. *Eur. Polym. J.* 1992, **28**, 505
27 Lairez, D., Emery, J. R., Durrand, D., Hayward, D. and Pethrick, R. A. *Plastics, Rubber Composites Process. Applicat.* 1991, **16**, 231
28 Elwell, R. J., Hayward, D. and Pethrick, R. A. *Plastics, Rubber Composites Process. Applicat.* 1992, **17**, 275
29 MacKinnon, A. J., Jenkins, S. D., McGrail, P. T. and Pethrick, R. A. *Macromolecules* 1992, **25**, 3492
30 McArdle, C. B., Burke, F. J. and McGettrick, B. P. *Plastics, Rubber Composites Process. Applicat.* 1991, **16**, 245
31 McGettrick, B. P. and Vij, J. K. *Ferroelectrics* 1992, **133**, 151
32 Kremer, F., Boese, D., Meier, G. and Fischer, E. W. *Prog. Coll. Polym. Sci.* 1989, **77**, 129
33 Krieble, V. *US Pat. 2895950* 1959
34 Stamper, D. J. *Br. Polym. J.* 1983, **15**, 34
35 Boeder, C. W. in 'Structural Adhesives—Chemistry and Technology' (Ed. S. R. Hartshorn), Plenum Press, New York, 1986, Ch. 5
36 Lees, W. A. *Br. Polym. J.* 1979, **11**, 64
37 Okamoto, Y. *J. Adhesion* 1990, **32**, 227, 237
38 Riew, C. K. and Gillham, J. K. (Eds) 'Rubber-Modified Thermoset Resins', Advances in Chemistry Series no. 208, American Chemical Society, Washington, DC, 1984
39 Riew, C. K. and Gillham, J. K. (Eds) 'Rubber-Toughened Plastics', Advances in Chemistry Series no. 222, American Chemical Society, Washington, DC, 1989
40 Daly, J. H., Pethrick, R. A., Fuller, R. A., Cunliffe, A. V. and Datta, P. K. *Polymer* 1981, **22**, 32
41 Daly, J. H. and Pethrick, R. A. *Polymer* 1981, **22**, 37
42 Daly, J. H. and Pethrick, R. A. *Polymer* 1982, **23**, 1619
43 Wagner, K. W. *Arch. Electrotech.* 1914, **2**, 371
44 Maxwell, J. C. 'Electricity and Magnetism', 3rd Edn, Oxford University Press, Oxford, 1892, p. 452
45 Scaife, B. K. P. 'Principles of Dielectrics', Clarendon Press, Oxford, 1989, Ch. 4
46 Bidstrup, W. W. and Senturia, S. D. *Polym. Eng. Sci.* 1989, **29**, 290
47 Scaife, W. G. S. in 'Complex Permittivity' (Ed. B. K. P. Scaife), English Universities Press, London, 1971, Ch. 2